Z. Kristallogr. Suppl. **26** (2007) 311-316

Mixed site occupancies in μ-Zr-Nb-Al by resonant powder diffraction

J.-M. Joubert[1,*], R. Černý[2], H. Emerich[3]

[1] LCMTR, CNRS, 2-8 rue Henri Dunant, F-94320 Thiais Cedex, France
[2] Laboratoire de Cristallographie, Université de Genève, 24 Quai E. Ansermet, CH-1211 Genève 4, Switzerland
[3] SNBL, ESRF, BP220, F-38043 Grenoble Cedex, FRANCE
[*] Contact author; e-mail: jean-marc.joubert@glvt-cnrs.fr

Keywords: Frank-Kasper, μ phase, intermetallic compounds, resonant powder diffraction, site occupancies, Rietveld analysis

Abstract. The ternary μ phase in the system Zr-Nb-Al has been studied by resonant powder diffraction at the Zr and Nb K-edges in order to determine the distribution of the three species on the five different sites of the crystal structure. The results are presented in comparison with those obtained for the μ phase in other systems. The comparison of the results obtained using two or three data sets in the refinement allows a discussion on the methodology.

Introduction

The μ phase is a hard-brittle intermetallic compound pertaining to the group of Frank-Kasper phases. It forms in 12 binary *A*-*B* systems where *A* is Nb, Ta, Mo or W and *B* is Fe, Co, Ni or Zn. For this reason, it shows up (and is deleterious because of its brittleness) in many technologically important systems such as *e.g.* Ni and Co superalloys. Five crystallographic sites are occupied by the different atoms in space group $R\bar{3}m$. In binary systems, it appears around the stoichiometric composition A_6B_7 but with wide homogeneity ranges which raise the question of the substitutional disorder necessary to accommodate the non-stoichiometry. This feature has been studied by Rietveld refinement [1] of the structure in several systems [2]. *A* atoms prefer the sites with high coordination numbers (CN14, CN15, CN16) and *B* those with low coordination numbers (two sites with CN12).

A ternary μ phase, not present in any of the binary systems, exists in the system Zr-Nb-Al around the composition $Zr_{30}Nb_{20}Al_{50}$ [3]. The distribution of the different atoms among the different sites is of particular interest since neither Zr nor Al forms a binary μ phase. For this ternary compound, this distribution cannot be simply obtained because (*i*) the substitutional disorder involves three atoms and at least two data sets in which the atomic contrast is different are necessary to refine the occupancy parameters, (*ii*) the disorder may occur on all the sites of the crystal structure, (*iii*) Zr and Nb present the particularity to have both similar atomic numbers (Z_{Zr}=40, Z_{Nb}=41) and Fermi lengths (b_{Zr}=7.16 fm, b_{Nb}=7.054 fm), (*iv*) isotopic substitution can neither be used due to the absence of contrasted isotopes. This makes

necessary the use of resonant diffraction (for a review see *e.g.* [4]). In the present work, the distribution of the three atoms among the five different sites was obtained from a joint Rietveld structural refinement using powder diffraction data collected at wavelengths close to Zr and Nb K-edges in addition to one data set collected at a wavelength far from the edge.

Experimental

The sample was synthesized by arc melting of the pure elements under pure argon atmosphere. An annealing treatment was performed during 27 days at 1100°C, the sample being wrapped in a tantalum foil to prevent contamination and sealed in a silica tube. The homogeneity and phase composition was checked by electron microprobe analysis (EPMA). The diffraction measurements were performed at the ESRF on the Swiss Norwegian Beamline at three selected wavelengths. The brittle sample was crushed in an agate mortar and was introduced in a glass capillary of diameter $2R$=0.3 mm. The geometry for the measurement was Debye-Scherrer with 6 detectors, each equipped with a silicon analyzer. The wavelength was selected by adjusting the Bragg angle of the Si-111 channel-cut monochromator. A first wavelength was chosen at λ=0.49997(1) Å far from two considered edges of Zr and Nb (measurement from 2 to 40°, step 0.005° (all the angles are given in units 2θ), 1.5 s/step).
For both measurements close to the absorption edge, the fluorescence (proportional to absorption) signal of the sample was recorded during an energy scan across the respective edges. The derivative of this signal was calculated and the edge was defined as the energy at which the first maximum of the derivative is observed. A second monochromator scan was then interrupted at the edge. The diffraction pattern of a silicon standard (SRM 640b) was then measured, and the wavelength refined gave the exact energy of the edge. A third monochromator scan was stopped approximately 8 eV before the edge and the energy was again precisely determined by a second silicon scan. The diffraction measurement of our sample was carried out at this energy. The energy offset between the edge and the energy of the measurement equals to the difference between the energies obtained by the two silicon scans. The maximum error is estimated to be 1 eV. On the other hand, the fluorescence signal from the energy scan around the edge was used to calculate f' and f'' of the resonant element with the program CHOOCH [5]. The dispersion values for the other elements were obtained from Cromer and Liberman [6, 7]. The uncertainty on the offset between the measurement and the edge energies induces an uncertainty on f' of the order of 0.1 e. The measurement at the Zr edge was done at λ=0.68914(2) Å (17991 eV, 7 eV before the edge) from 3 to 57° (step 0.005°, 2 summed scan with acquisition time 1.1 s/step). The one at the Nb edge was performed at λ=0.65329(1) Å (18979 eV, 9 eV before the edge) from 3 to 54° (step 0.005°, 2 summed scan with acquisition time 1.2 s/step). The $m\mu R$ values (μ is the linear absorption coefficient, m is the powder packing factor ~0.3) was 0.82 (λ~0.5 Å), 0.32 (Zr-edge) and 1.11 (Nb-edge) and were taken into account in the refinement.
The refinement was performed with the program Fullprof [8] in the multi-pattern mode either using two or three patterns as explained in the following attributing equal weights to the different patterns. The background was interpolated between peaks. Slight asymmetry at very low angle was corrected. The second phase was refined with its own crystal structure [9]. As explained afterwards, the peaks of a third phase could not be indexed and were placed in excluded regions. For the μ phase, the variable coordinates and two displacement parameters

(one for the sites of coordination 12, one for the sites of higher coordination) were refined. The occupancy parameters of the three atoms were refined on the five sites of the crystal structure with the constraints that no vacancies are present and that the global composition matches the analyzed composition. This leaves two unknowns per site in four sites *i.e.* eight variables. The procedure for establishing such constraints in Rietveld refinement programs has been discussed in [10].

Results

Three phases are evidenced in the examination of the microstructure of the sample on back-scattered electron images. From the EPMA, the composition of the μ phase was determined to be $Zr_{35(1)}Nb_{15(1)}Al_{50(1)}$. A second phase of composition $Zr_{\sim 38}Nb_{\sim 20}Al_{\sim 42}$ could be identified as the ternary extension of the binary phase Zr_4Al_3. A third phase of composition $Zr_{\sim 40}Nb_{\sim 23}Al_{\sim 36}$ was evidenced and assimilated to the X phase reported by Hansen *et al.* [3]. It gives numerous peaks that could not be indexed *ab initio*. The phase could neither be identified as being isostructural to any known intermetallic phase. We verified that none of the additional peaks could be indicative of a simple superstructure of the μ phase. Excluded regions were defined to eliminate these peaks from the refinement.
The dispersion curves are displayed in figure 1. As expected for an intermetallic compound, the positions of the edges are found in good agreement with those of the pure metals.

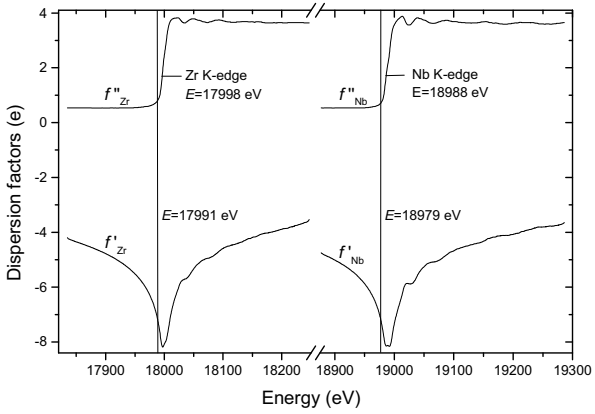

Figure 1. Dispersion parameters as obtained from the fluorescence measurement and calculation by CHOOCH [5]. The vertical lines and corresponding energies indicate the energies of the measurements at the Zr and Nb-edges.

The values of the dispersion parameters used in this work are listed in table 1. A definition of the scattering contrast has been provided by Zhang *et al.* [11]. Though this definition is not perfect (it leads to severe inconsistencies in the case of neutron diffraction when one scattering length is positive and the other negative), it has been used to present the scattering con-

trast between Zr and Nb in the different experiments of this study (figure 2). As expected the contrast is large and opposite in the two experiments close to the edges, it is larger at the Zr K-edge because Zr has the lower atomic number and it increases strongly with the angle.

Table 1. Dispersion parameters (in e) of the different elements in the different experiments.

	f'_{Zr}	f''_{Zr}	f'_{Nb}	f''_{Nb}	f'_{Al}	f''_{Al}
λ=0.49997 Å	-0.256	2.18	-0.422	2.375	0.0320	0.0310
K_{Zr}	-7.29	0.82	-2.54	0.589	0.0560	0.0520
K_{Nb}	-2.04	3.35	-7.15	0.70	0.0560	0.0520

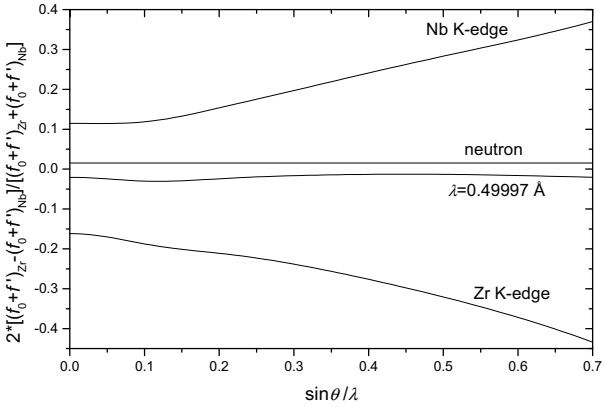

Figure 2. Contrast factor between Zr and Nb at the three energies used in this work. The value obtained in a fictive neutron experiment is shown for comparison.

In principle, two patterns for which the contrasts between the atoms are different are sufficient to solve the problem of determining the site occupancies. In order to test the dependency of the results on the number of patterns used, four different combinations of patterns were tested. The obtained occupancy parameters are presented in table 2. For comparison purposes, the occupancy parameters were not constrained to be positive. In the final refinement done with the three patterns, the results of which are presented in table 3, the negative occupancy parameters were set to zero and the refinement was conducted with fewer variables. An example of calculated and observed patterns is presented in figure 3.

Discussion

In the case of the binary μ phase, the site occupancies have already been rationalized in terms of the tendency for large, *d*-electron poor elements (so-called *A* elements) to prefer the sites of high coordination [2]. The site occupancies may however vary to accommodate the particular stoichiometry of the phase in the homogeneity range. Ternary phases allow a more

subtle classification if two *A* or two *B* elements are both present. This is clearly the case in μ Zr-Nb-Al. The Al atoms are ordered on the two sites of CN12 showing a strong *B* character.

*Table 2. Results of the refinements in four different schemes. Results are given in number of atoms per site. Al complement Zr and Nb on each site to full occupancy. The occupancy parameters were not constrained to be positive. Occupancies on site 18*h *complement the number of each atom to match the analyzed composition.*

site	λ~0.5 Å/Zr K-edge	λ~0.5 Å/Nb K-edge	Zr/Nb K-edges	three patterns
3*a*	$Zr_{-0.01(16)}Nb_{0.19(12)}Al_{2.82}$	$Zr_{0.07(15)}Nb_{0.16(16)}Al_{2.77}$	$Zr_{0.04(9)}Nb_{0.15(7)}Al_{2.81}$	$Zr_{0.03(9)}Nb_{0.17(8)}Al_{2.80}$
6c_1	$Zr_{5.71(22)}Nb_{0.56(17)}Al_{-0.27}$	$Zr_{5.28(21)}Nb_{0.95(23)}Al_{-0.23}$	$Zr_{5.49(12)}Nb_{0.70(10)}Al_{-0.19}$	$Zr_{5.53(13)}Nb_{0.67(11)}Al_{-0.20}$
6c_2	$Zr_{5.97(20)}Nb_{0.39(16)}Al_{-0.36}$	$Zr_{5.81(20)}Nb_{0.48(21)}Al_{-0.29}$	$Zr_{5.88(11)}Nb_{0.46(9)}Al_{-0.34}$	$Zr_{5.87(12)}Nb_{0.46(10)}Al_{-0.33}$
6c_3	$Zr_{2.03(22)}Nb_{4.12(17)}Al_{-0.15}$	$Zr_{1.76(20)}Nb_{4.38(22)}Al_{-0.14}$	$Zr_{1.87(12)}Nb_{4.24(10)}Al_{-0.11}$	$Zr_{1.92(13)}Nb_{4.20(11)}Al_{-0.12}$
18*h*	$Zr_{-0.05}Nb_{0.59}Al_{17.46}$	$Zr_{0.73}Nb_{-0.12}Al_{17.39}$	$Zr_{0.37}Nb_{0.30}Al_{17.33}$	$Zr_{0.30}Nb_{0.35}Al_{17.35}$

Table 3. Final results from the Rietveld refinement of μ Zr-Nb-Al (composition: $Zr_{35(1)}Nb_{15(1)}Al_{50(1)}=Zr_{13.65}Nb_{5.85}Al_{19.5}$): a=5.3089(1) Å, c=28.837(1) Å, s.g. $R\bar{3}m$, R_B=7.7% (0.5 Å), 7.9% (K_{Zr}), 8.9% (K_{Nb}), χ^2=2.1 (0.5 Å), 3.9 (K_{Zr}), 2.0 (K_{Nb}). Due to the way the constraints are established, it is not possible to give the esd's for the occupancy parameters constrained to the variables

site	composition	*x*	*y*	*z*	*B*
3*a* (CN12)	$Zr_{0.26(10)}Nb_{0.05(8)}Al_{2.69}$	0	0	0	0.81(5)
6c_1 (CN15)	$Zr_{5.20(10)}Nb_{0.80(10)}$	0	0	0.16624(7)	0.28(2)
6c_2 (CN16)	$Zr_{5.26(9)}Nb_{0.74(9)}$	0	0	0.35096(8)	0.28(2)
6c_3 (CN14)	$Zr_{1.75(9)}Nb_{4.25(9)}$	0	0	0.45624(6)	0.28(2)
18*h* (CN12)	$Zr_{1.18}Nb_{0.01}Al_{16.81}$	0.83421(46)	-*x*	0.25529(12)	0.81(5)

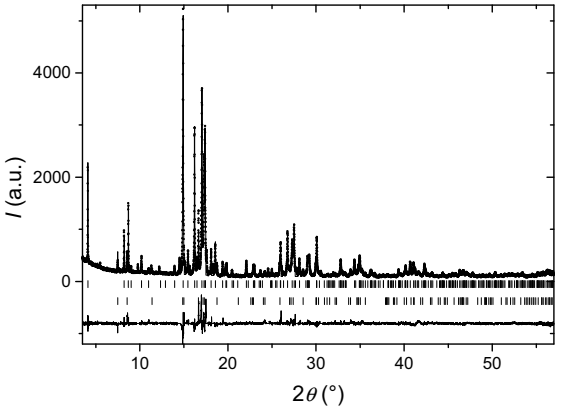

Figure 3. Observed (.) pattern at the Zr-K edge together with the pattern calculated from the refined structural model of μ-Zr-Nb-Al (-) and difference curve. Reflection positions are indicated as vertical lines.

However, the two *A* elements do not share equally the sites of high coordination since Zr among these sites prefer these of the highest coordinations. Our results may be compared with the previous study of the ternary μ Nb-V-Ni and μ Nb-Ni-Al [12], and the tendency towards more and more affinity to the low coordination sites may be rationalized as follows: Zr→Nb→V→Al→Ni. Except for the peculiar case of Al, which is not a transition element but which behaves so, the classification follows the decrease of the atomic radius and the increase in the number of *d*-electrons.

Mathematically, the problem of determining the site occupancies can be solved by the only use of two patterns. Even with the use of three patterns it is not possible to either refine vacancies or suppress the composition constraint. It yields too many variables. Due to the fact that atoms are in principle, mixed on all the sites of the crystal structure, the scale factor has to be fixed by the number of electron either in the cell or at one given site. The results are similar when either λ~0.5 Å/Zr K-edge or λ~0.5 Å/Nb K-edge patterns are used. This indicates the good consistency of the results and confirms that the dispersion parameters close to the edges have been accurately determined in the two cases. The similar estimated standard deviations (esd's) observed are also an indication that the refinement at the Nb edge has not been much affected by the weaker contrast and lower quality data due to Zr absorption.

The refinements using either the two patterns at Zr and Nb edges or the three patterns together give virtually the same results and esd's, showing that the pattern measured at λ~0.5 Å is redundant. The increase of statistics made by collecting a supplementary pattern has negligible effect since the information it provides is only on the Al which is anyhow very well contrasted in the two other patterns. In these two cases the esd's are reduced by a factor of two as regards the refinement with λ~0.5 Å/Zr K-edge or λ~0.5 Å/Nb K-edge patterns, but the results are equivalent. This is due to better use of the contrast factor, and to the fact that the contrast is reversed between the Zr K-edge Nb K-edge patterns.

References

1. Rietveld, H. M., 1969, *J. Appl. Crystallogr.*, **2**, 65–71.
2. Joubert, J.-M. & Dupin, N., 2004, *Intermetallics*, **12**, 1373-1380.
3. Hansen, R. C. & Raman, A., 1970, *Z. Metallkde.*, **61**, (2), 115-120.
4. Hodeau, J.-L., Favre-Nicolin, V., Bos, S., Renevier, H., Lorenzo, E. & Berar, J.-F., 2001, *Chem. Rev.*, **101**, 1843-1867.
5. Evans, G. & Pettifer, R. F., 2001, *J. Appl. Crystallogr.*, **34**, 82-86.
6. Cromer, D. T. & Liberman, D. A., 1970, *J. Chem. Phys.*, **53**, 1891-1898.
7. Cromer, D. T. & Liberman, D. A., 1981, *Acta Crystallogr.*, **A37**, 267-268.
8. Rodríguez-Carvajal, J., 1990, *XV Congress of Int. Union of Crystallography, Satellite Meeting on Powder Diffraction*, 127.
9. Wilson, C. G., Thomas, D. K. & Spooner, F. J., 1960, *Acta Crystallogr.*, **13**, 56-57.
10. Joubert, J.-M., Cerný, R., Latroche, M., Percheron-Guégan, A. & Yvon, K., 1998, *J. Appl. Crystallogr.*, **31**, 327-332.
11. Yuegang Zhang, Wilkinson, A. P., Nolas, G. S., Lee, P. L. & Hodges, J. P., 2003, *J. Appl. Crystallogr.*, **36**, 1182-1189.
12. Joubert, J.-M., 2005, *J. Solid State Chem.*, **178**, 1620-1629.